Assessing Hurricane Rainfall Mechanisms Using a Physics-Based Model: Hurricanes Isabel (2003) and Irene (2011)

Ping Lu, Ning Lin, Kerry Emanuel,
Daniel Chavas and James Smith 2018

Speaker: 陳威縉
Adviser: 楊明仁教授
Date: Oct. 30, 2018

1. **Introduction**
2. TCR Model
3. Model Evaluation
4. Rainfall Mechanisms
5. Sensitivity Analysis
6. Summary

Introduction

- Tropical Cyclone Rainfall (TCR) Model:
  1) Initially developed by Emanuel et al. (2008) as part of a synthetic approach for estimating TC hazard.
  2) Zhu et al. (2013) first described the rainfall algorithm and investigated the model's ability to capture the overall statistics of TC rainfall.
- Other TC rainfall models:
  1) Rainfall Climatology and Persistence (R-CLIPER) Model (Lonfat et al. 2004; Tuleya et al. 2007).
  2) Parametric Hurricane Rainfall Model (PHRaM) (Lonfat et al. 2007).
  3) Modified Smith for Rainfall (MSR) Model (Langousis and Veneziano 2009a).

Introduction

- Clear physic-based framework, the rainfall is related to upward vapor flux:
  1) Frictional convergence.
  2) Changes in the axisymmetric vorticity of the gradient wind (vortex spinup and spindown, stretching).
  3) Interaction of the storm with topography and large-scale baroclinity (wind shear).
- Weather and Research Forecasting (WRF) Model-generated storm wind characteristics and environment as input for TCR.

Cases

Cat. 5 Hurricane Isabel (2003)

Cat. 3 Hurricane Irene (2011)

Riverine floods induced by Irene over the Delaware River basin (red arrows) are estimated by coupling TCR and WRF with a hydrological model.

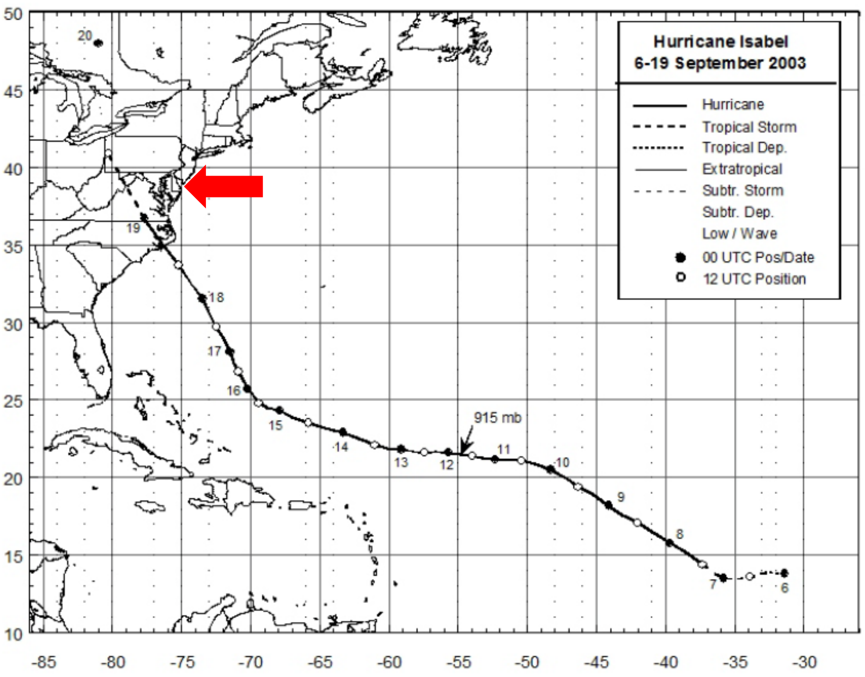

Figure 1. Best track positions for Hurricane Isabel, 6-19 September 2003.

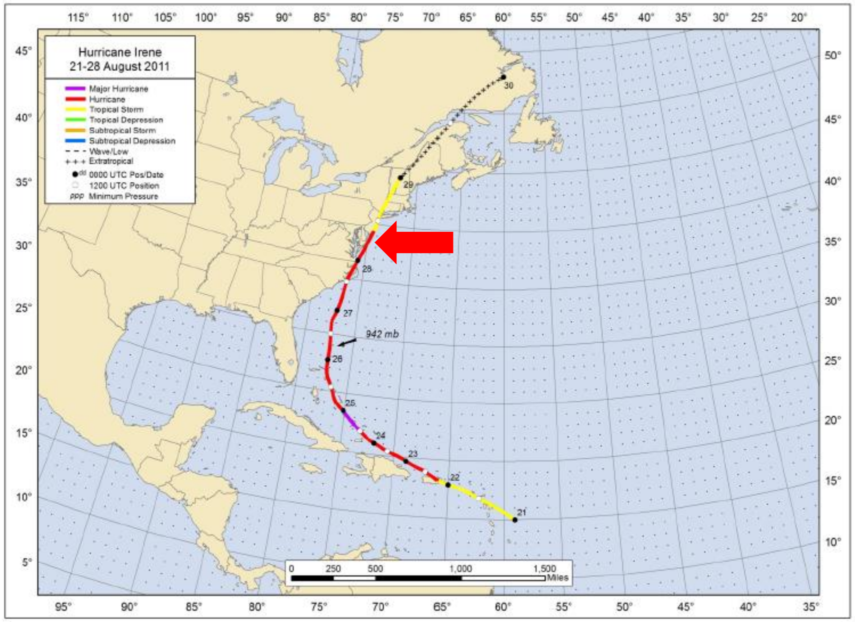

Figure 1. Best track positions for Hurricane Irene, 21 -28 August 2011. Track during the extratropical stage is based on analyses from the NOAA Hydrometeorological Prediction Center.

Source:
Tropical Cyclone Report Hurricane Isabel (AL132003), National Hurricane Center.
Tropical Cyclone Report Hurricane Irene (AL092011), National Hurricane Center.

1. Introduction
2. TCR Model
3. Model Evaluation
4. Rainfall Mechanisms
5. Sensitivity Analysis
6. Summary

Precipitation Rate & Vertical Velocity

$$\boxed{P_{rate} = \varepsilon_p \frac{\rho_{air}}{\rho_{liquid}} q_s w \cdots (1)}$$

ε_p = 0.9 … precipitation efficiency;
ρ_{air} … density of water vapor;
ρ_{liquid} … density of liquid water (ρ_{air} / ρ_{liquid} = 0.0012);
q_s … saturation specific humidity (at the storm center at 900 mb);
w ($w > 0$)… vertical velocity.

$$\boxed{w = w_f + w_h + w_t + w_s + w_r \cdots (13)}$$

w_f … frictional component;
w_h … topographic component;
w_t … stretching component;
w_s … baroclinic/shear component;
w_r (= -0.005 m/s) … radiative cooling component.

Radial Advection of Angular Momentum & Frictional Torque

$$\boxed{u\frac{\partial M}{\partial r} \cong -r\frac{\partial \tau_\theta}{\partial z} \cdots (2)}$$

(Ooyama 1969; Kepert 2001, 2003)

u … radial velocity;
r … radius from the storm center;
M … absolute angular momentum (per unit mass);
τ_θ … azimuthal turbulent stress.

$$\boxed{M = rV + \frac{1}{2} fr^2}$$

V … azimuthal wind speed;
f … Coriolis parameter.

Vertical Velocity: Frictional Component

From mass continuity eq. (assuming incompressible flow):

$$\boxed{\frac{\partial w}{\partial z} = -\frac{1}{r}\frac{\partial}{\partial r}\left(ru\right) = \frac{1}{r}\frac{\partial}{\partial r}\left(r^{2}\,\frac{\partial \tau_{\theta} / \partial z}{\partial M / \partial r} \right) \cdots (3),(4)}$$

Then integrating vertically through the depth of the boundary layer:

$$\boxed{w_{f} = \int_{w_h}^{w_b} \frac{\partial w'}{\partial z} dz = -\frac{1}{r}\frac{\partial}{\partial r}\left(r^{2}\,\frac{\tau_{\theta s}}{\partial M / \partial r} \right) \cdots (6)}$$

w_b … vertical velocity at the top of the boundary layer;
w_h … surface vertical velocity;
$\tau_{\theta s}$ … azimuthal surface stress.

$$\boxed{\tau_{\theta s} = -C_{d} \left| \vec{V} \right| V \cdots (8)}$$

C_d … drag coefficient;
V … total surface wind.

Vertical Velocity: Topographic Component

Surface vertical velocity:

$$\boxed{w_h = \vec{V} \cdot \nabla h \cdots (7)}$$

V … horizontal wind velocity ($|V| \geq$ threshold V_{th});
h … topographical height.

Elevation map at 0.25° x 0.25 ° resolution.

The vertical velocity at the top of the boundary layer is topographic and frictional components combined:

$$\boxed{w_b = w_h + w_f \cdots (5)}$$

Vertical Velocity: Stretching Component

Above the boundary layer conservation of angular momentum (vertical advection neglected) gives:

$$\boxed{u = -\frac{\partial M/\partial t}{\partial M/\partial r} \cdots (9)}$$

Integrating mass continuity eq. up from the top of the boundary layer:

$$\boxed{\frac{\partial w}{\partial z} = -\frac{1}{r}\frac{\partial}{\partial r}(ru) = \frac{1}{r}\frac{\partial}{\partial r}\left(r\frac{\partial M/\partial t}{\partial M/\partial r} \right)}$$

$$\boxed{w_t = \int_b^H \frac{1}{r}\frac{\partial}{\partial r}\left(r\frac{\partial M/\partial t}{\partial M/\partial r} \right) dz \cong H_b \frac{1}{r}\frac{\partial}{\partial r}\left(r\frac{\partial M/\partial t}{\partial M/\partial r} \right) \cdots (11)}$$

H_b (= H-b) = 1 km … representative depth scale of the lower troposphere.

Interaction of the Vortex with the Saturation Entropy Surfaces

In a coordinate system moving with the storm center:

$$\boxed{\vec{V} \cdot \nabla s^* + w \frac{\partial s^*}{\partial z} = 0 \cdots (A1)}$$

$s*$ … saturation moist entropy;
V … total vector horizontal wind relative to the moving storm.

$$\boxed{\frac{\partial s^*}{\partial z} \cong (1 - \varepsilon_p) \frac{\partial s_d}{\partial z} = (1 - \varepsilon_p) \frac{c_p}{g} N^2 \cdots (A2)}$$

(Emanuel et al. 1994)

ε_p … precipitation efficiency;
s_d … entropy od dry air;
c_p … heat capacity of dry air;
g … acceleration of gravity;
N … buoyancy frequency of dry air.

Interaction of the Vortex with the Saturation Entropy Surfaces

Rewriting (A1) with (A2) as:

$$\boxed{w \cong -\frac{g}{c_p}\frac{\vec{V}\cdot\nabla s^*}{\left(1-\varepsilon_p\right)N^2}\cdots(A3)}$$

Isentropic ascent and descent.

$$\boxed{\vec{V}\cdot\nabla s^* = \left(\vec{V}_e+\vec{V}_{TC}\right)\cdot\nabla\left(s_e{}^*+s_{TC}{}^*\right)\cdots(A4)}$$

subscript *e* refers to environment;
subscript *TC* refers to tropical cyclone.

$$\boxed{\vec{V}\cdot\nabla s^* = \cancel{\vec{V}_e\cdot\nabla s_e{}^*}+\vec{V}_e\cdot\nabla s_{TC}{}^*+\vec{V}_{TC}\cdot\nabla s_e{}^*+\cancel{\vec{V}_{TC}\cdot\nabla s_{TC}{}^*}}$$

$$\boxed{\vec{V}\cdot\nabla s^* \cong \vec{V}_e\cdot\nabla s_{TC}{}^*+\vec{V}_{TC}\cdot\nabla s_e{}^*\cdots(A5)}$$

Interaction of the Vortex with the Saturation Entropy Surfaces

$$\boxed{\nabla s_e{}^{*} = \frac{f}{T_s - T_t} \hat{k} \times \Delta \vec{V}_e \cdots (A6)}$$

(Emanuel 1995)

$$\boxed{\nabla s_{TC}{}^{*} = \frac{-\hat{j}V}{T_s - T_t} \left(\frac{V}{r} + \frac{\partial V}{\partial r} \right) \cdots (A7)}$$

(Emanuel 1986)

f … Coriolis parameter;
T_s … surface temperature;
T_t … tropopause temperature;
k … unit vector in the vertical direction;
ΔV_e … vector wind shear across the troposphere;
j … unit vector in the radial direction;
V … azimuthal gradient wind.

Vertical Velocity: Baroclinic/Shear Component

Taking:

$$\boxed{\vec{V}_e \cong \Delta\vec{V}_e} \quad \boxed{\vec{V}_{TC} \cong V\left(\hat{k}\times\hat{j}\right)}$$

Rewriting (A3) with (A5)-(A7) as:

$$\boxed{w_s \cong \frac{g}{c_p\left(T_s - T_t\right)\left(1-\varepsilon_p\right)N^2} V\left(f + \frac{V}{r} + \frac{\partial V}{\partial r}\right)\left(\Delta\vec{V}_e \cdot \hat{j}\right)\cdots(A8,12)}$$

ΔV_e is estimated from the difference of the geostrophic wind V_g at 200 and 850 mb ($V_{g,200mb}$ - $V_{g,850mb}$).

Precipitation Rate & Vertical Velocity

In and above the boundary layer:

$$\boxed{w_b = w_h + w_f \cdots (5)}$$

$$\boxed{w_H = w_b + w_t \cdots (10)}$$

All components combined:

$$\boxed{w = w_H + w_s + w_r = w_f + w_h + w_t + w_s + w_r \cdots (13)}$$

Thus,

$$\boxed{P_{rate} = \varepsilon_p \frac{\rho_{air}}{\rho_{liquid}} q_s \left(w_f + w_h + w_t + w_s + w_r \right) \cdots (14)}$$

If $w < 0$ (downward motion), the precipitation rate is set to zero.

1. Introduction
2. TCR Model
3. **Model Evaluation**
4. Rainfall Mechanisms
5. Sensitivity Analysis
6. Summary

Model Evaluation

- Advanced Research version of WRF (ARW) ver. 3.4.1.
- Scheme:
  Single-moment 6-class microphysics scheme
  Yonsei University planetary boundary layer scheme
  Monin-Obukhov surface-layer scheme
  Noah land surface scheme
  Dudhia shortwave scheme
  Rapid Radiative Transfer Model longwave scheme
- WRF simulations start about 18 hr before landfall.
- Three nested domains are used, hourly outputs from the second domain (horizontal grid size = 4 km).
- Outputs:
  Track, wind and specific humidity (storm center) at 900 mb (gradient level), environmental wind shear (between 850 and 200 mb, averaged over the 200-500-km annulus from the storm center).

3a. Radial Distribution of Azimuthally Averaged Rainfall

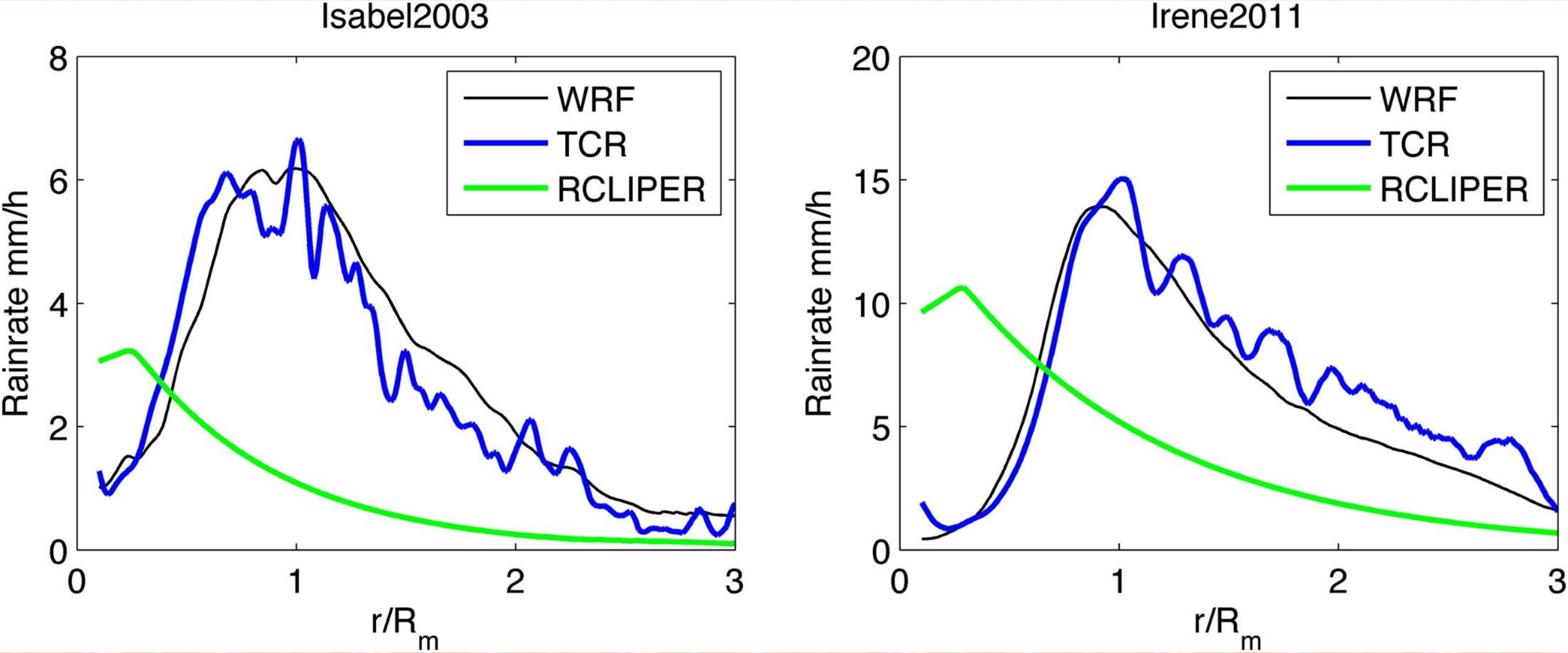

Fig. 1

Rainfall Profiles which are averaged over 18 hr during and after landfall.

R_m … radius of maximum wind.

3b. Spatial Distribution of Rainfall

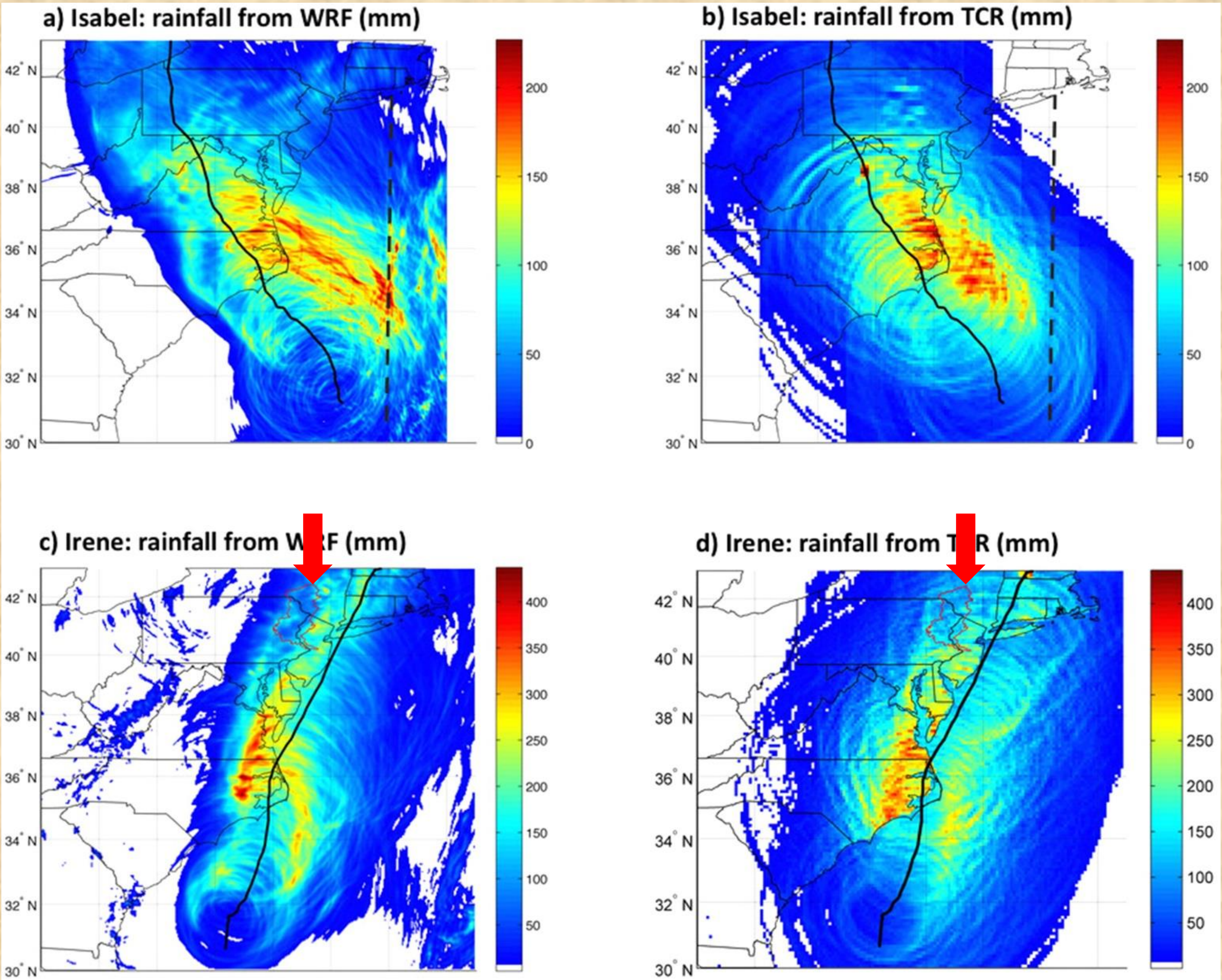

Fig. 2
Accumulation Rainfall (mm)

The dashed lines indicate the same reference location (Long Island).

The red polygons indicate the boundary of Deleware River basin.

3c. Flood Peaks in the Delaware River Basin

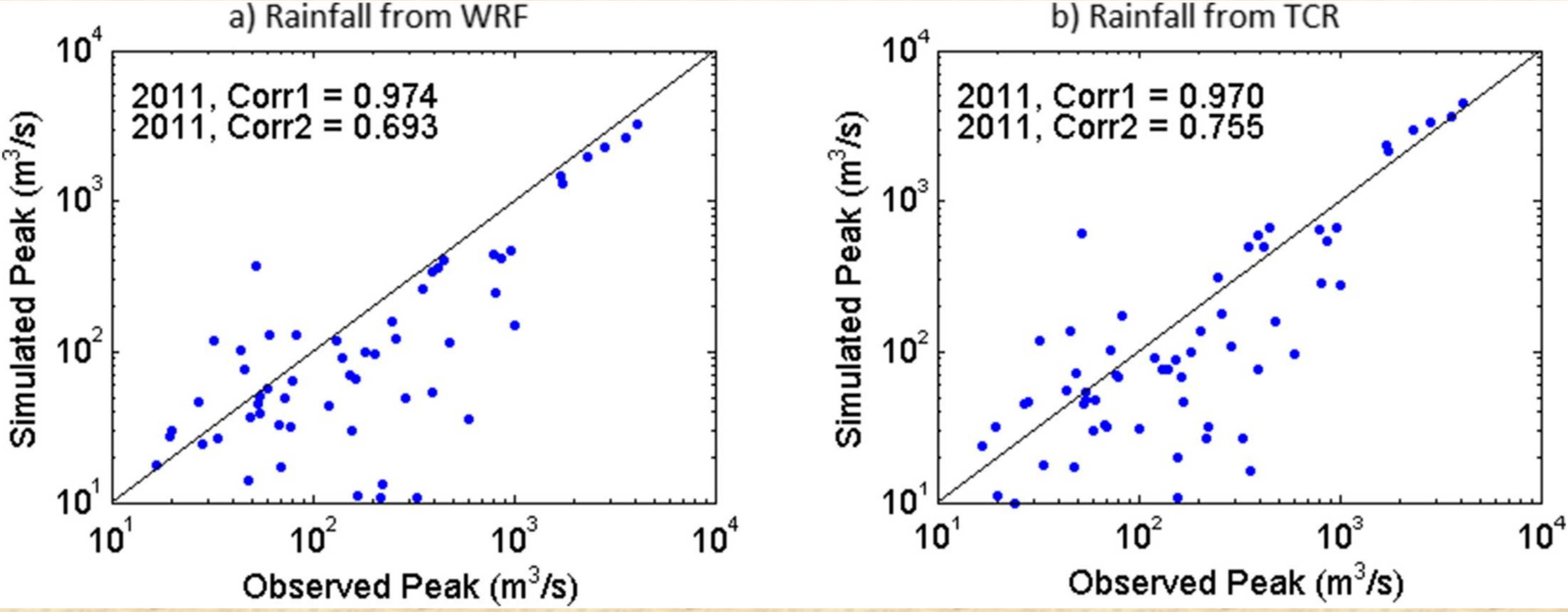

Fig. 3 Comparison of simulated (CUENCAS hydrologic model) vs. observed flood peaks at 67 USGS stream gauging stations in the Delaware River basin for Hurricane Irene (2011).

Corr1 … Pearson correlation in normal scale.

Corr2 … in log scale.

1. Introduction
2. TCR Model
3. Model Evaluation
4. Rainfall Mechanisms
5. Sensitivity Analysis
6. Summary

4a. P_{rate}-wq_s Relationship

- Rainfall P_{rate} is estimated by the upward vapor flux wq_s at a reference height.
- Neglecting local evaporation, change in the total column atmospheric water content due to horizontal advection and horizontal movement of raindrops.
- $q \approx q_s$

4a. P_{rate}-wq_s Relationship

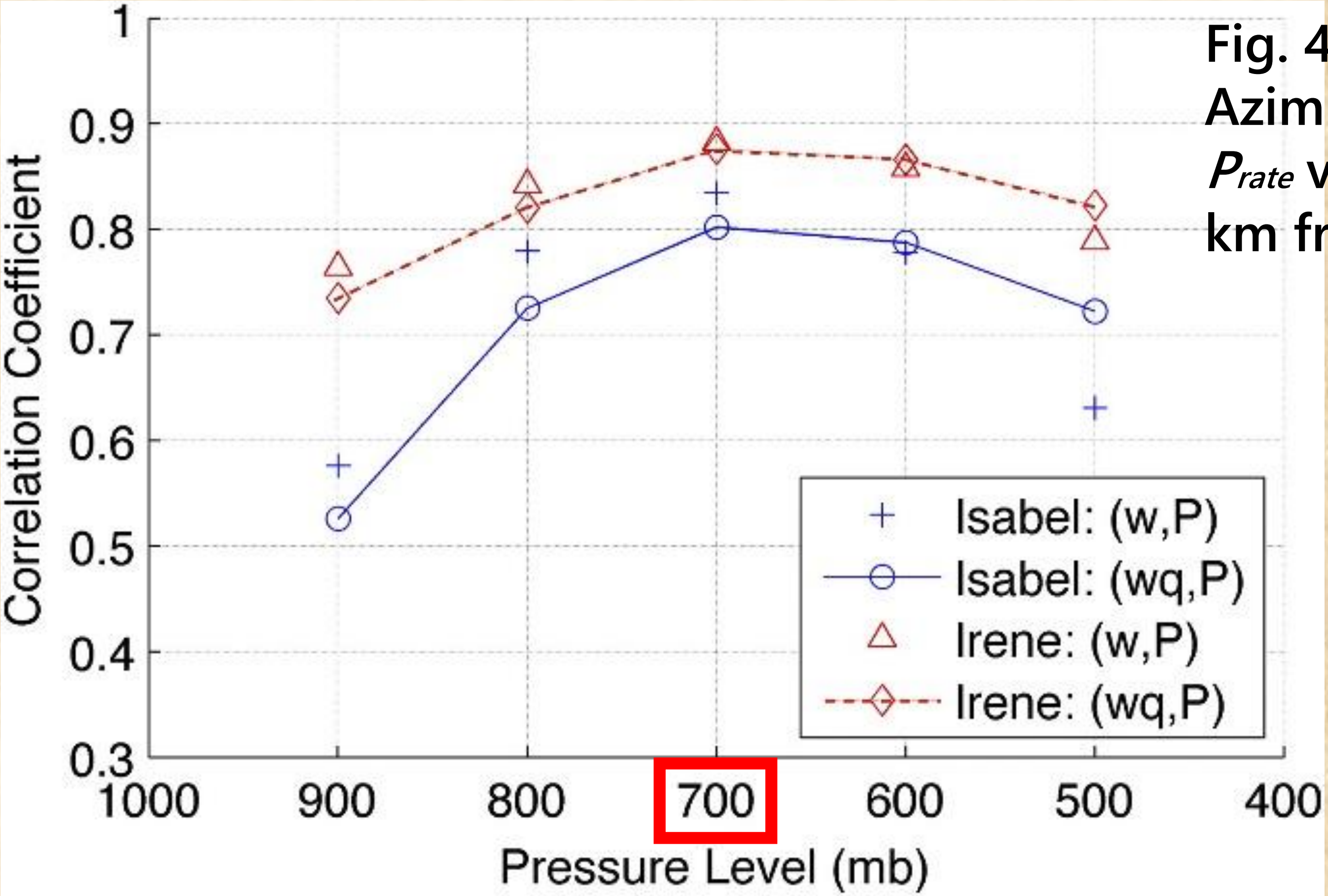

Fig. 4
Azimuthally Averaged P_{rate} vs. wq within 600 km from Storm Center.

4a. P_{rate}-wq_s Relationship

Fig. 5
Rainfall (mm)
(a) - (c): Isabel
(d) - (e): Irene

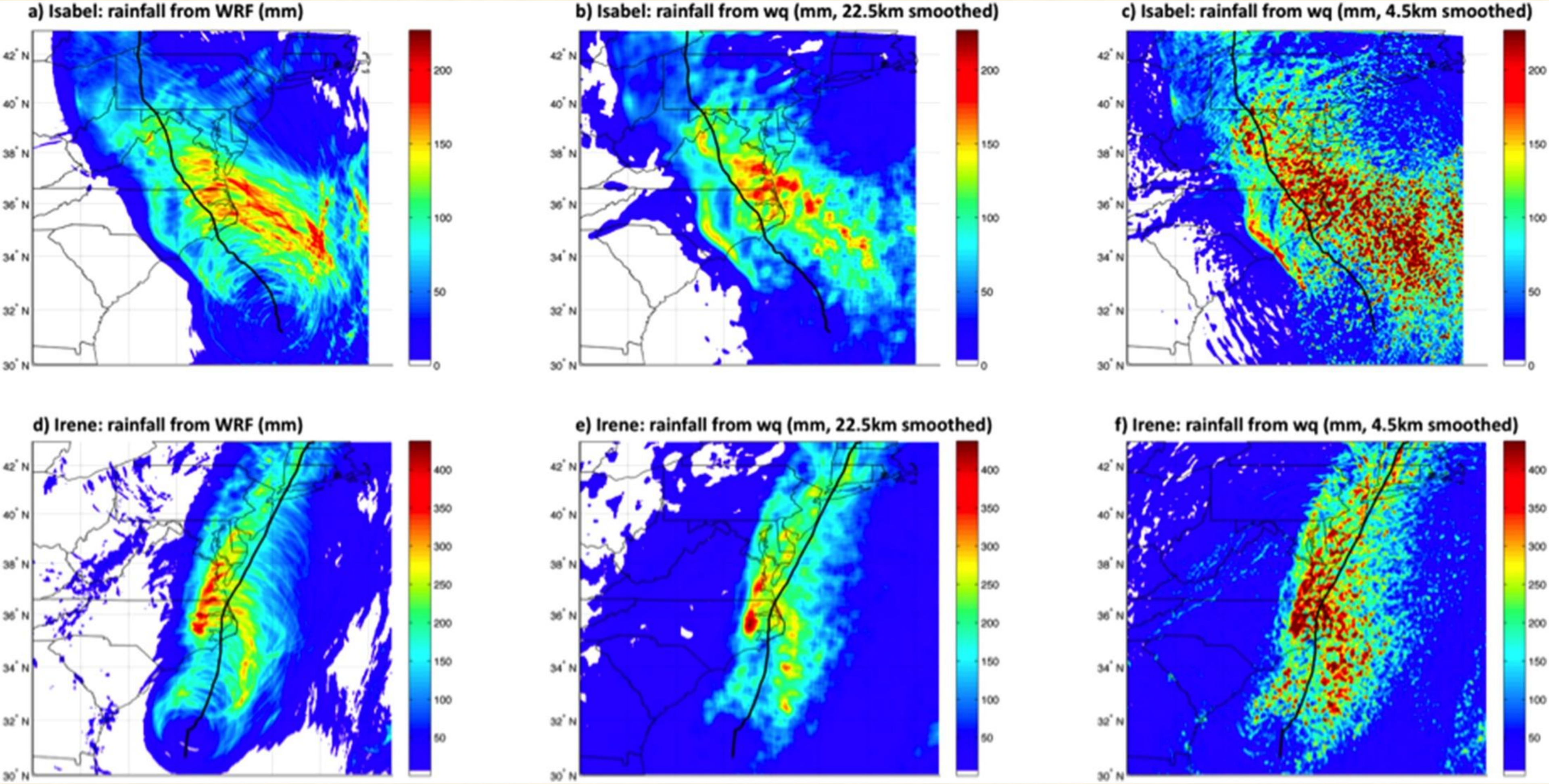

a) Isabel: rainfall from WRF (mm)

b) Isabel: rainfall from wq (mm, 22.5km smoothed)

c) Isabel: rainfall from wq (mm, 4.5km smoothed)

d) Irene: rainfall from WRF (mm)

e) Irene: rainfall from wq (mm, 22.5km smoothed)

f) Irene: rainfall from wq (mm, 4.5km smoothed)

WRF ⟷ From *wq* (22.5/4.5 km Smoothed)

4c. Rainfall Decomposition

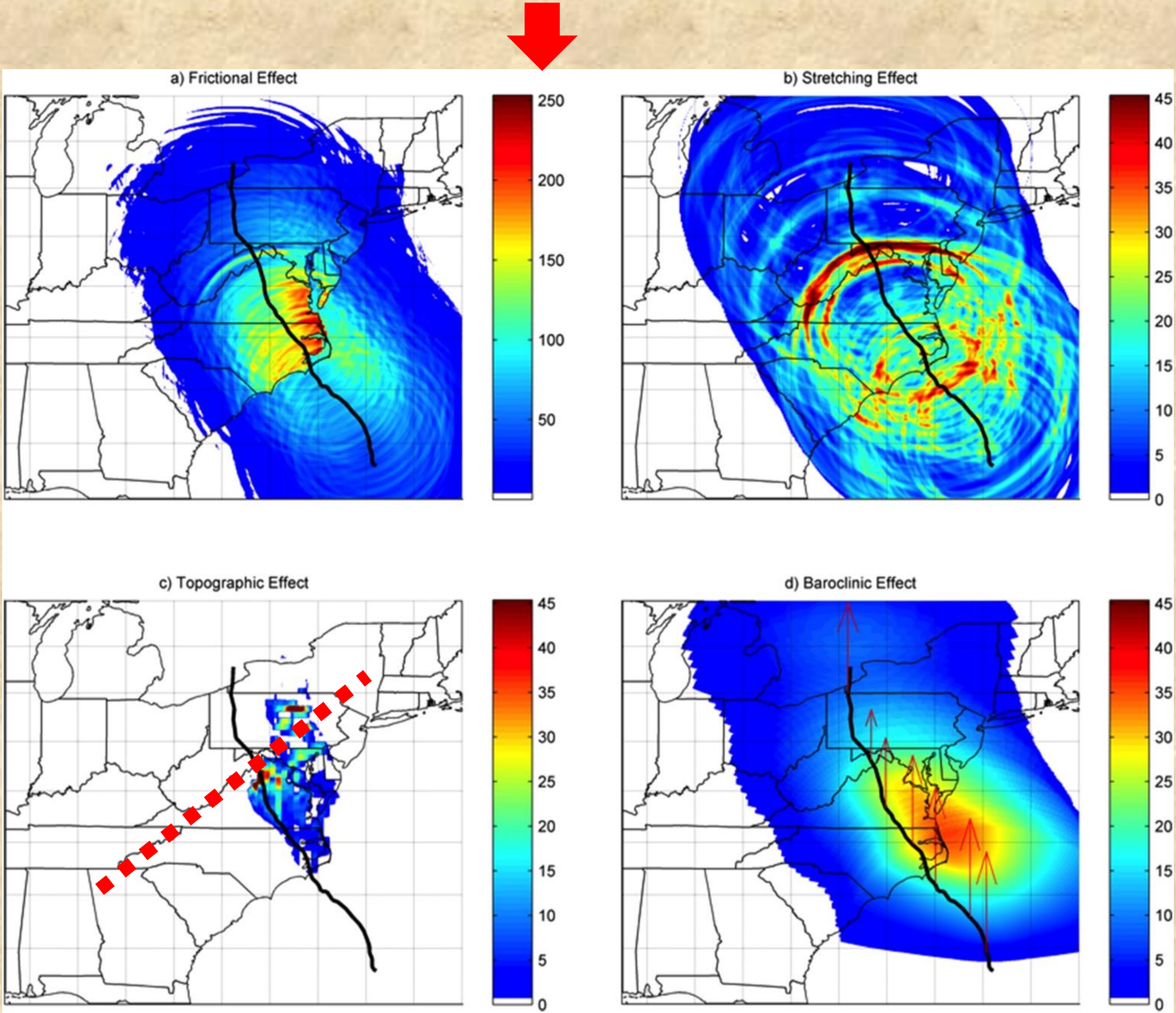

Fig. 6
Isabel

Rainfall (mm) by
a) Frictional
b) Stretching
c) Topographic
d) Baroclinic
Effect.

Arrows:
Environmental
Wind Shear

4c. Rainfall Decomposition

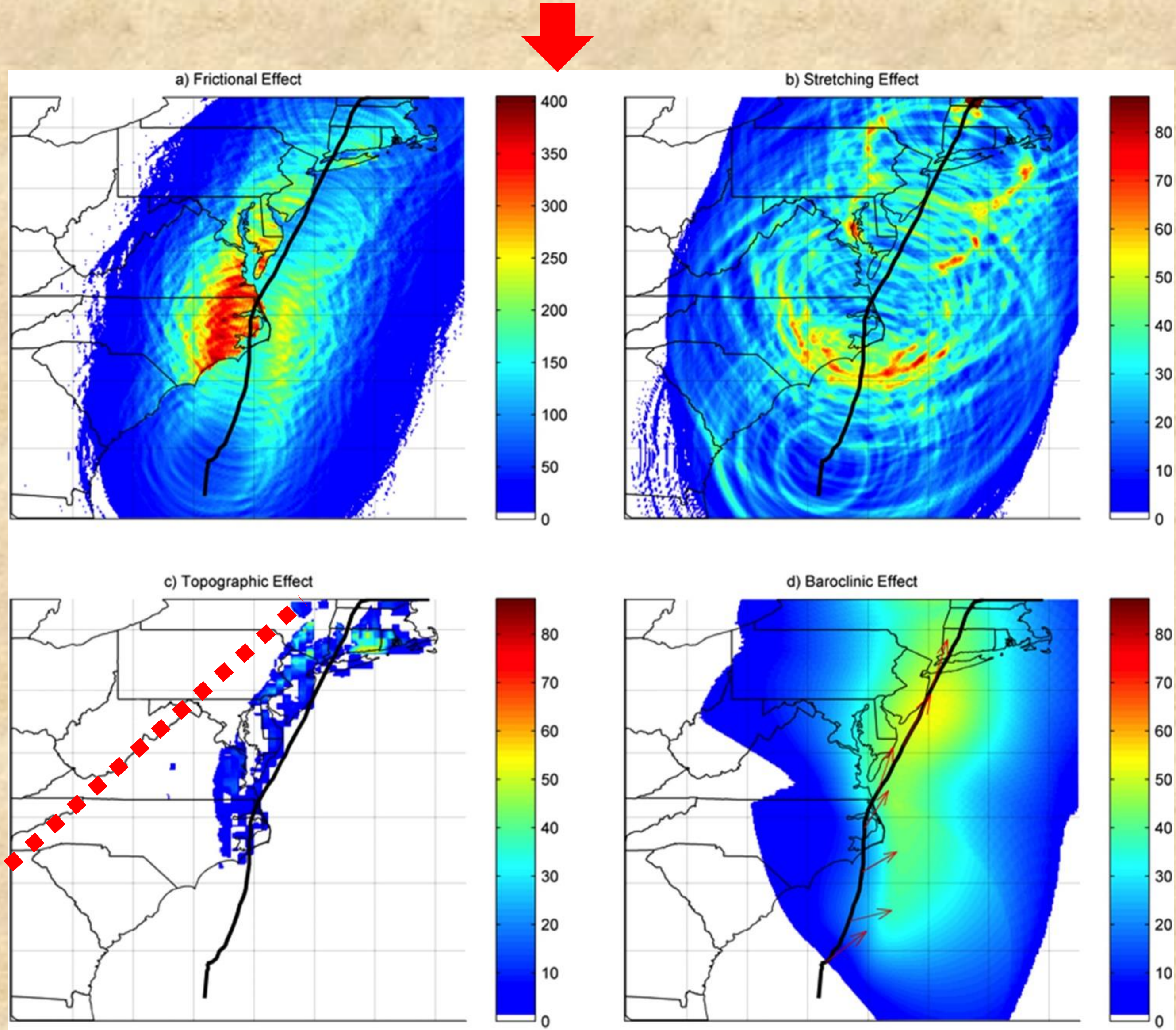

Fig. 7
Irene

Rainfall (mm) by
a) Frictional
b) Stretching
c) Topographic
d) Baroclinic
Effect.

Arrows:
Environmental
Wind Shear

4c. Rainfall Decomposition

- **Frictional Effect:**
  Frictional-convergence term dominates.

$$\boxed{w_f = -\frac{1}{r}\frac{\partial}{\partial r}\left(r^2\frac{\tau_{\theta s}}{\partial M/\partial r}\right)\cdots(6)}$$

- **Stretching Effect:**
  Ring-shaped rainfall distribution at large radius indicates the weakening of the storm (decreasing of intensity and increasing of radius of maximum wind).

$$\boxed{w_t \cong H_b\frac{1}{r}\frac{\partial}{\partial r}\left(r\frac{\partial M/\partial t}{\partial M/\partial r}\right)\cdots(11)}$$

Isabel
Irene

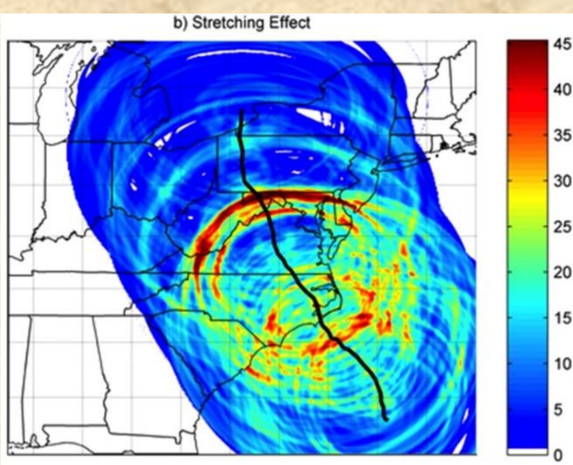

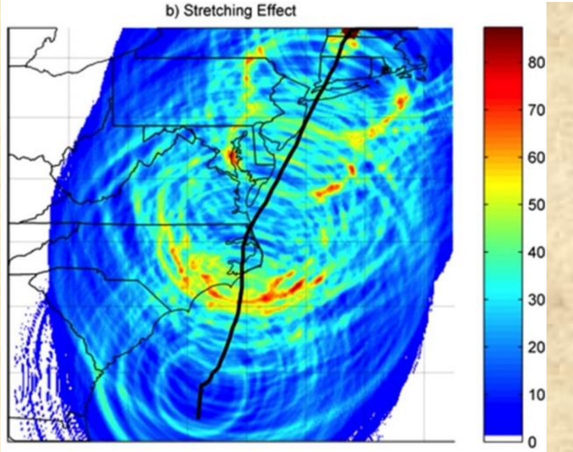

4c. Rainfall Decomposition

- Topographic Effect:

$$\boxed{w_h = \vec{V} \cdot \nabla h \cdots (7)}$$

- Underestimated rainfall in mountainous regions:
  1) where drag coefficient is bigger (Garratt 1977);

$$\boxed{\tau_{\theta s} = -C_d \left|\vec{V}\right| V \cdots (8)}$$

  2) orographic lifting is associated with increased precipitation efficiency (Huang et al. 2014).

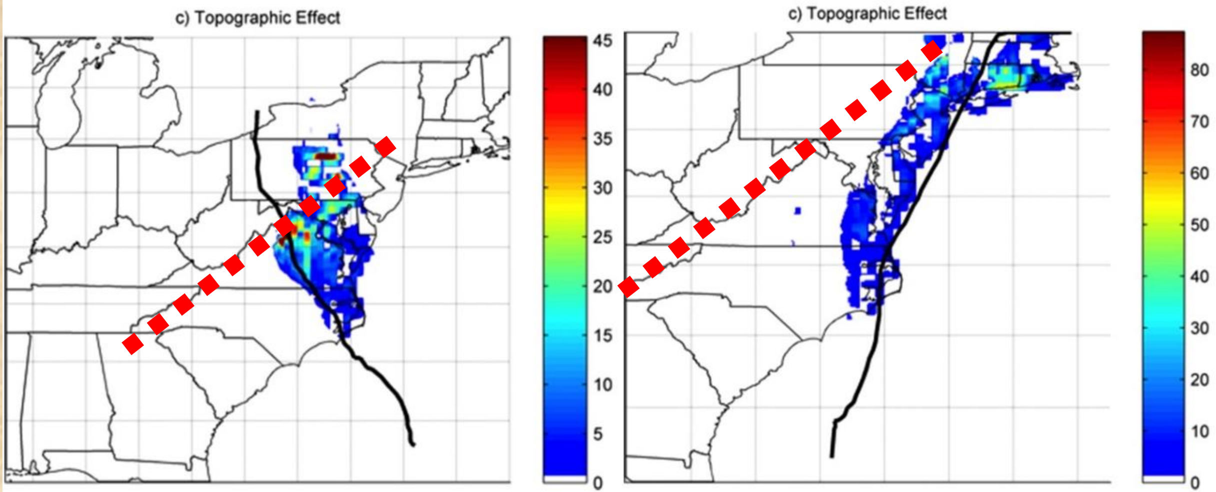

Isabel / Irene

4c. Rainfall Decomposition

- **Baroclinic Effect:**
  Downshear Direction

$$w_s \cong \frac{g}{c_p\left(T_s - T_t\right)\left(1-\varepsilon_p\right)N^2} V\left(f + \frac{V}{r} + \frac{\partial V}{\partial r}\right)\left(\Delta\vec{V}_e \cdot \hat{j}\right) \cdots (12)$$

Isabel / Irene

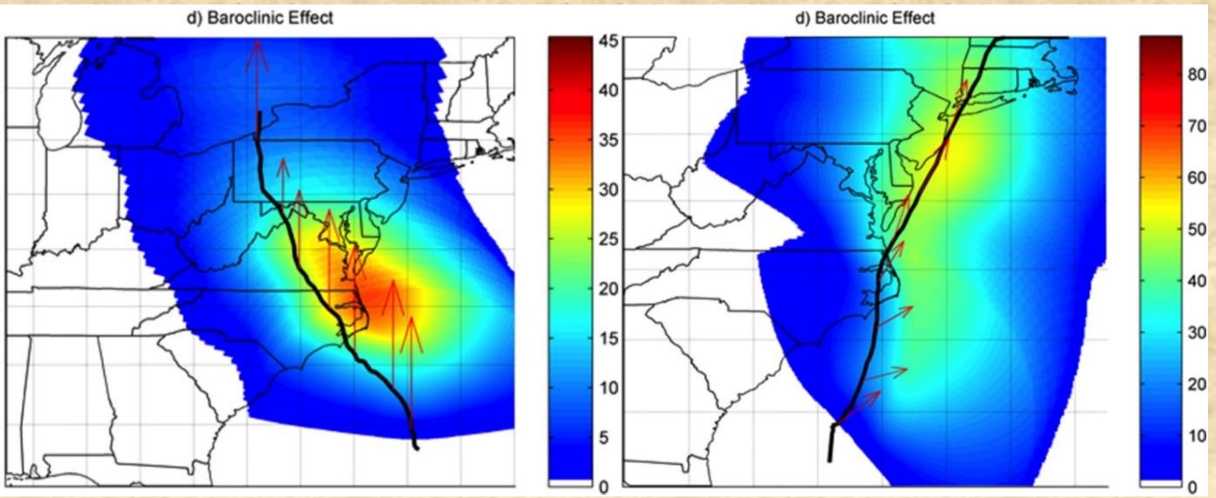

1. Introduction
2. TCR Model
3. Model Evaluation
4. Rainfall Mechanisms
5. **Sensitivity Analysis**
6. Summary

5. Sensitivity Analysis

a. Sensitivity to Gradient Wind
b. Sensitivity to Surface Drag Coefficient C_d
c. Sensitivity to the Topographic Wind Threshold V_{th}

5. Sensitivity Analysis

a. **Sensitivity to Gradient Wind**
b. Sensitivity to Surface Drag Coefficient C_d
c. Sensitivity to the Topographic Wind Threshold V_{th}

1) Smoothing of Numerical Wind Profiles from WRF

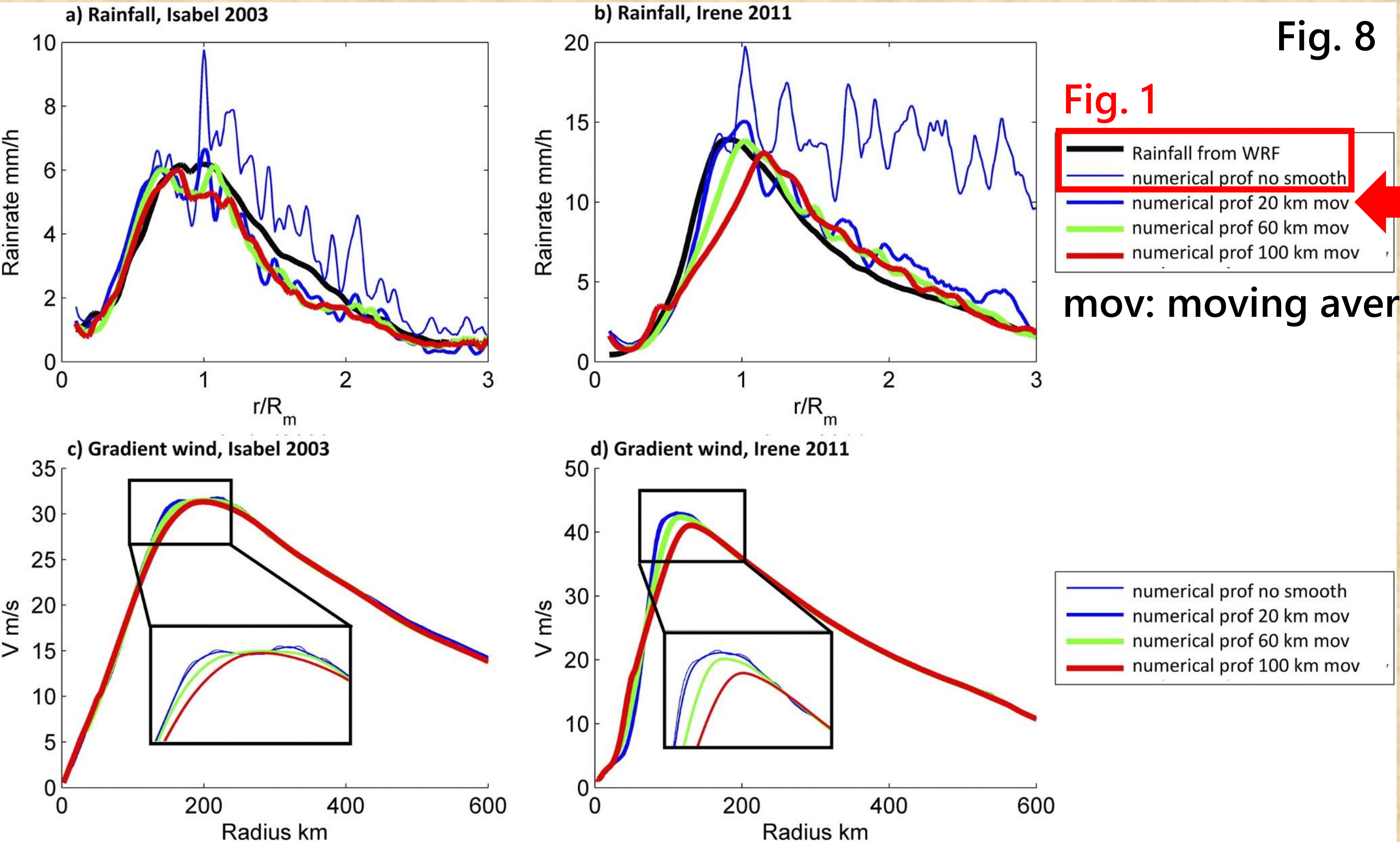

Fig. 8

Fig. 1

mov: moving average

1) Smoothing of Numerical Wind Profiles from WRF

TCR is highly sensitive to gradient wind because of time and radial derivatives of the angular momentum in w_f and w_t.

$$\boxed{w_f = -\frac{1}{r}\frac{\partial}{\partial r}\left(r^2 \frac{\tau_{\theta s}}{\partial M / \partial r}\right) \cdots (6)}$$

$$\boxed{w_t \cong H_b \frac{1}{r}\frac{\partial}{\partial r}\left(r \frac{\partial M / \partial t}{\partial M / \partial r}\right) \cdots (11)}$$

Rainfall estimation to small oscillations in angular momentum comes from neglecting nonlinear advection terms, which acts as a spatial filter with scale of ~20 km.

2) Analytical Wind Profiles

- Holland 1980, hereafter H80:
  The gradient wind balance and empirical exponential distribution of storm pressure.
- Emanuel 2004, hereafter E04:
  The free-tropospheric thermodynamic balance and boundary layer Ekman dynamic balance (Outer); boundary layer angular momentum balance and entropy quasi-equilibrium (Inner).
- Emanuel and Rotunno 2011, hereafter ER11:
  Improved solution for the inner region that arises from stratification of the outflow due to Kelvin-Helmholtz turbulence.
- Chavas et al. 2015, hereafter C15:
  Mathematically merges the <u>inner</u> region of <u>ER11</u> and the <u>outer</u> region of <u>E04</u>.
- Outer … nonconvecting region;
  Inner … convecting region, still outside the eyewall.

2) Analytical Wind Profiles

Fig. 9

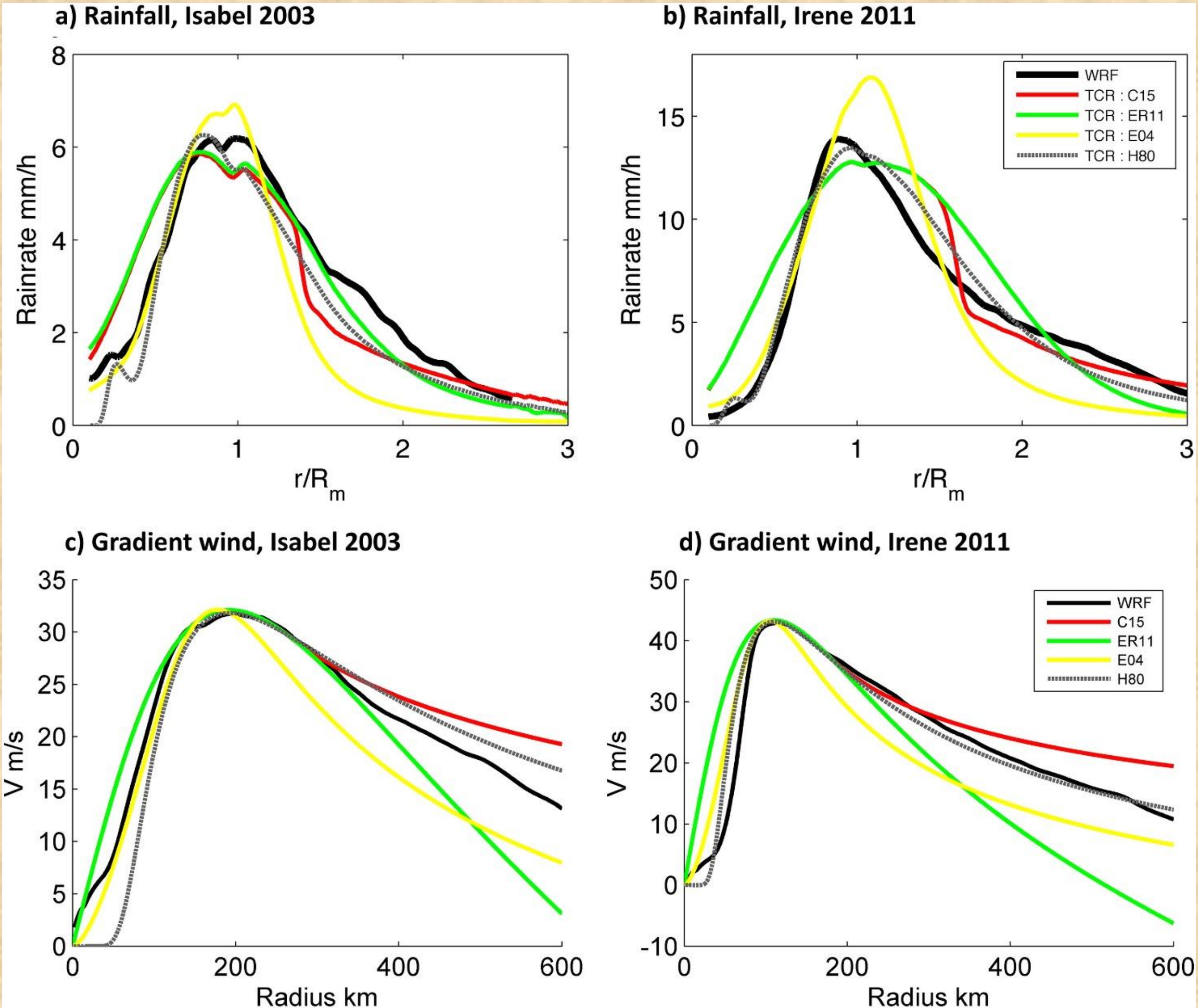

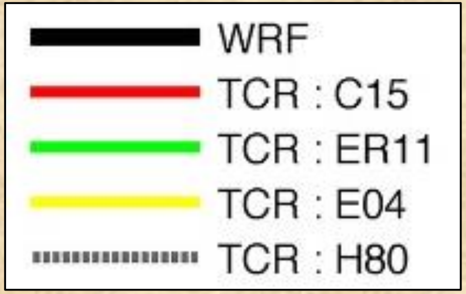

2) Analytical Wind Profiles

H80 **E04** **ER11** **C15**

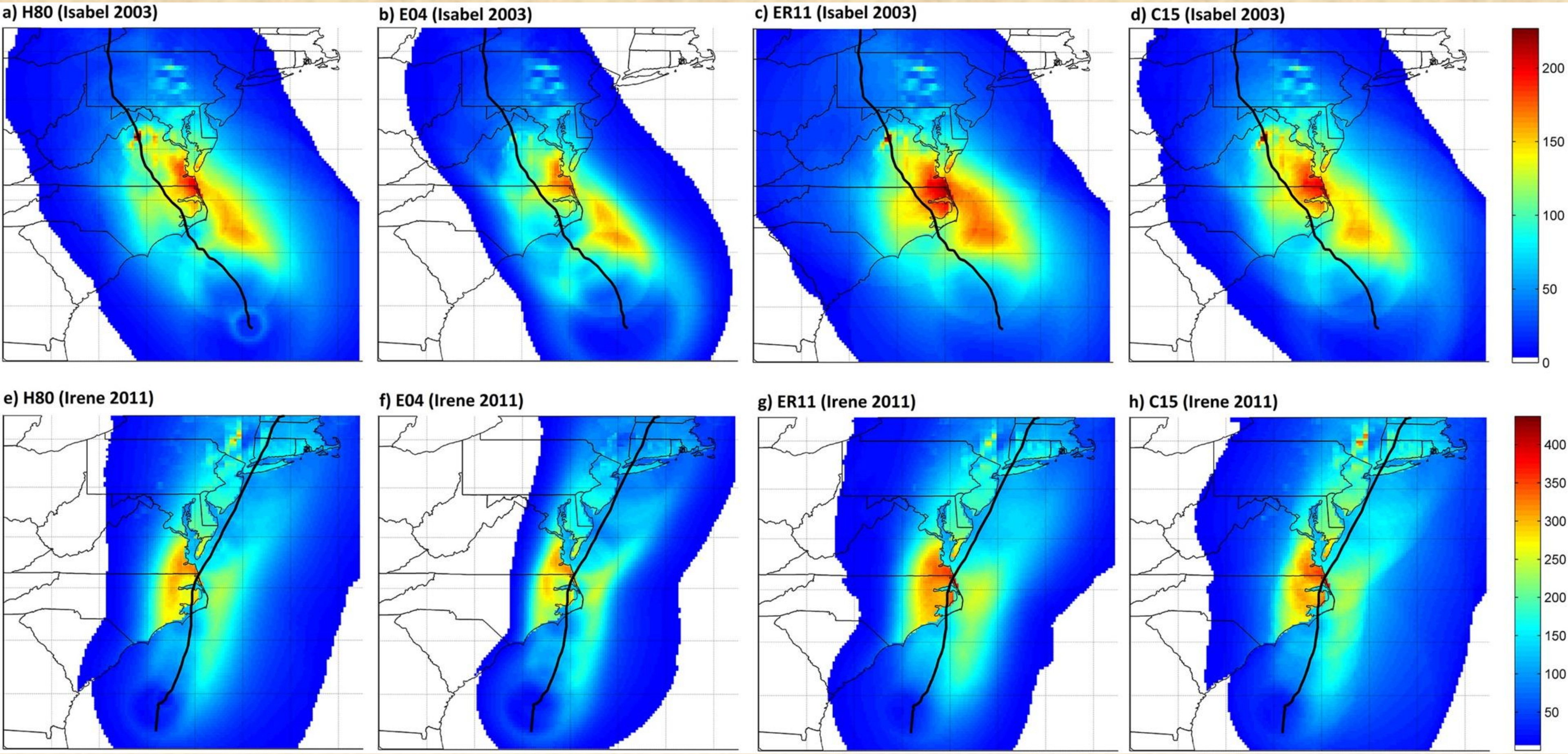

Fig. 10 Comparison of total rainfall accumulation (mm) estimated by TCR with different analytical wind profiles.

5. Sensitivity Analysis

a. Sensitivity to Gradient Wind

b. Sensitivity to Surface Drag Coefficient C_d

c. Sensitivity to the Topographic Wind Threshold V_{th}

5b. Sensitivity to Surface Drag Coefficient C_d

The drag coefficient (dimensionless):
Land surface (flat): 0.002;
Land surface (low-relief topography): 0.003 (Garratt 1977, not used);
Over the ocean: 0.001-0.002 (a function of wind speed).

Used as a tuning parameter.

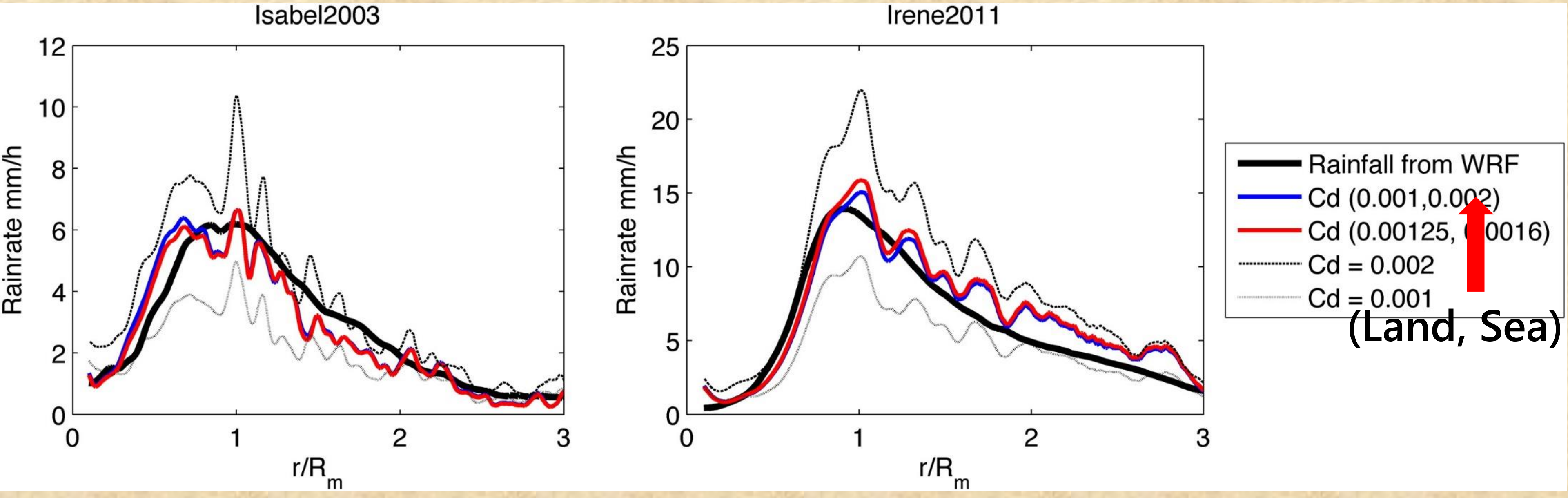

(Land, Sea)

Fig. 11 Red line of Isabel and blue line of Irene are same as in Fig. 1.

5b. Sensitivity to Surface Drag Coefficient C_d

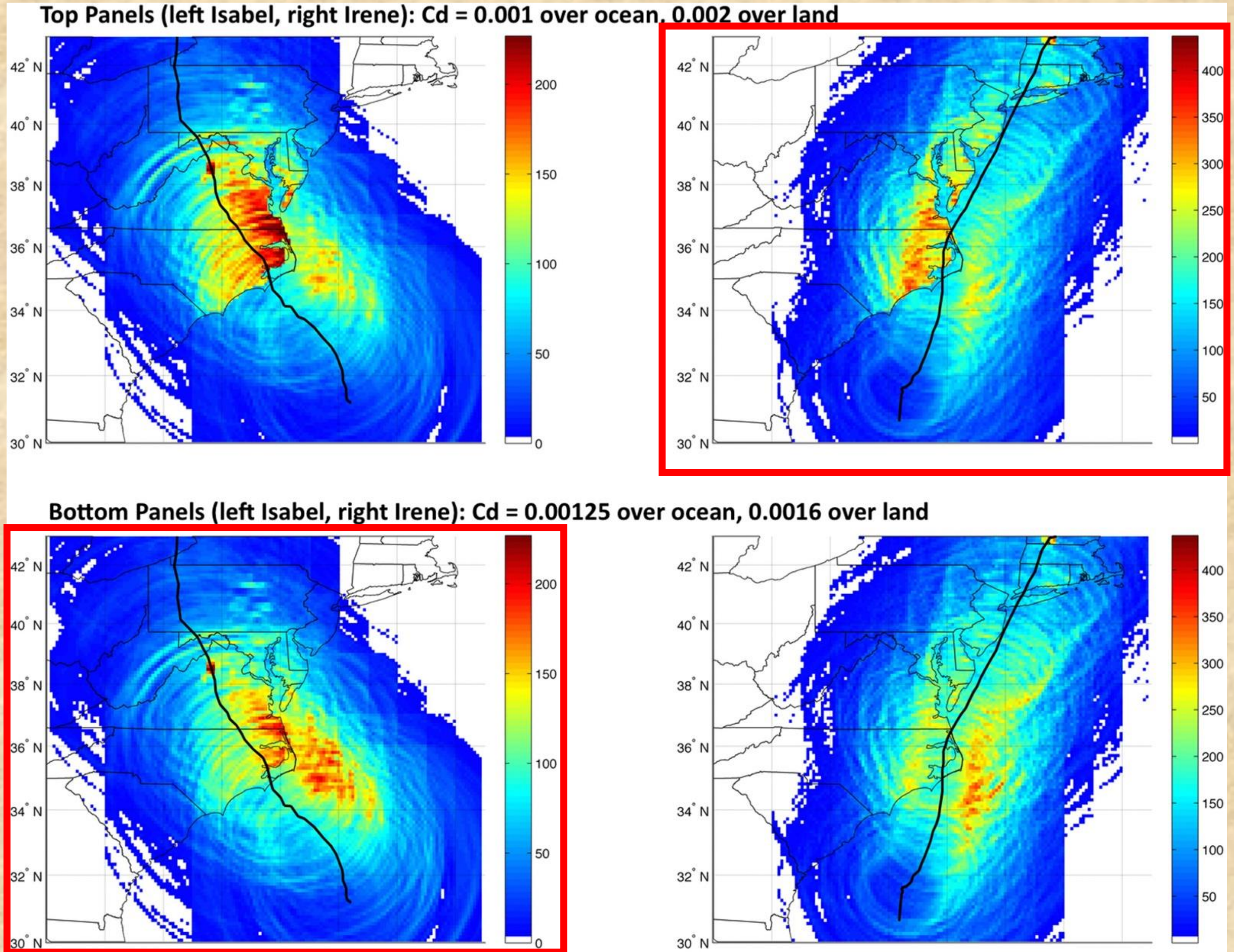
Top Panels (left Isabel, right Irene): Cd = 0.001 over ocean, 0.002 over land

Bottom Panels (left Isabel, right Irene): Cd = 0.00125 over ocean, 0.0016 over land

Fig. 12 Comparison of total rainfall accumulation (mm) from TCR with different drag coefficient.

5. Sensitivity Analysis

a. Sensitivity to Gradient Wind
b. Sensitivity to Surface Drag Coefficient C_d
c. Sensitivity to the Topographic Wind Threshold V_{th}

5c. Sensitivity to the Topographic Wind Threshold V_{th}

Without a sufficient wind threshold, TCR overestimates rainfall in the Appalachian regions.

Froude number:

$$\boxed{Fr = \frac{U}{NH}}$$

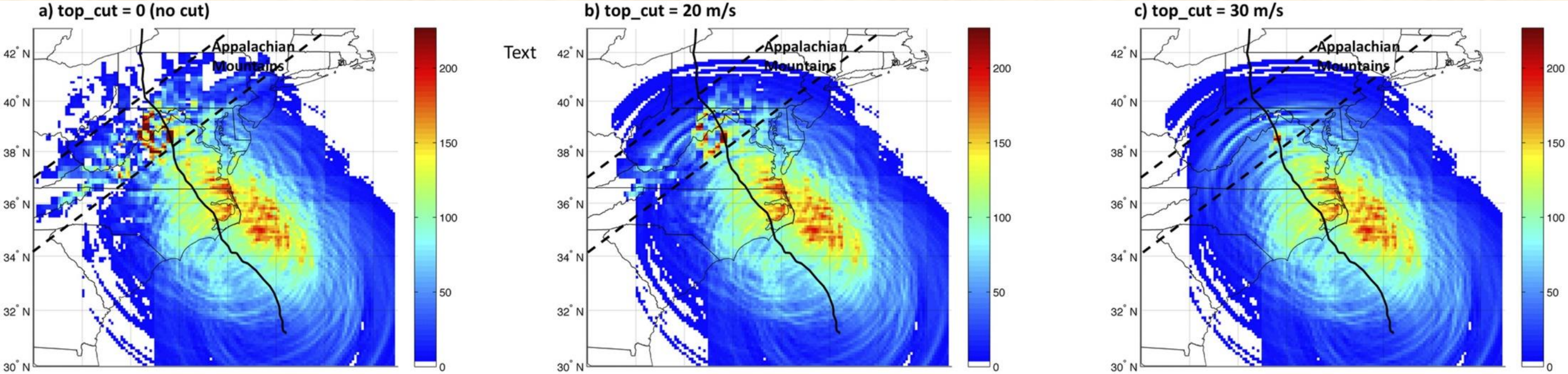

Fig. 13
Comparison of total rainfall accumulation (mm) from TCR for Isabel with different cutoff thresholds: (a) no cut, (b) 20, and (c) 30 m/s .

1. Introduction
2. TCR Model
3. Model Evaluation
4. Rainfall Mechanisms
5. Sensitivity Analysis
6. Summary

Summary

- TCR model is a fast algorithm that generates rainfall fields that compared well with WRF, and that generates flood peaks with a hydrologic model as accurately as WRF.
- Four major rainfall mechanisms of TCR model:
  1) Surface frictional convergence (dominant)
  2) Vortex stretching
  3) Interaction with topography
  4) Interaction with large-scale baroclinity (wind shear)

Summary

- Sensitivity analysis:
  1) Sensitive to the wind input: 20-km smoothing, and wind profiles from different model
  2) Sensitive to the drag coefficient (used as a tuning parameter)
  3) Cutoff wind threshold (30 m/s)
- Future improvements:
  1) Redistribution rainfall (horizontal movement of raindrops)
  2) Coupling TCR with boundary layer modeling (friction)
  3) Spatial and temporal variations of precipitation efficiency and humidity
  4) Variations at small spatial scale

References

- Beven, J., & Cobb, H. (2004). Tropical Cyclone Report Hurricane Isabel. *National Hurricane Center*, 16.
- Emanuel, K. A. (1986). An air-sea interaction theory for tropical cyclones. Part I: Steady-state maintenance. *Journal of the Atmospheric Sciences*, 43(6), 585-605.
- Emanuel, K. A. (1995). On thermally direct circulations in moist atmospheres. *Journal of the atmospheric sciences*, 52(9), 1529-1534.
- Lixion, A. A., & Cangialosi, J. (2011). Tropical Cyclone Report Hurricane Irene (AL092011). *National Hurricane Center*.
- Reinecke, P. A., & Durran, D. R. (2008). Estimating topographic blocking using a Froude number when the static stability is nonuniform. *Journal of the Atmospheric Sciences*, 65(3), 1035-1048.

Thanks for you listening.